Progress In Electromagnetics Research B, Vol. 23, 69–82, 2010

EXACT ELECTROMAGNETIC FIELD EXCITED BY A VERTICAL MAGNETIC DIPOLE ON THE SURFACE OF A LOSSY HALF-SPACE

M. Parise

University Campus Bio-Medico of Rome
Via Alvaro del Portillo 21, 00128 Rome, Italy

Abstract—A rigorous analytical procedure is developed that allows the exact evaluation of the complete integral representations for the time-harmonic electromagnetic (EM) field components generated by a vertical magnetic dipole (VMD) lying on the surface of a flat and homogeneous lossy half-space. Closed-form expressions for the radial distributions of the EM field components induced on the surface of the half-space are provided in terms of exponential functions and modified Bessel functions. Such expressions make it possible to overcome the limitations implied by the previously published quasi-static solutions, which are valid only in the low-frequency range. Numerical results are presented to show where the quasi-static approximations deviate from the exact solutions for a given homogeneous medium as frequency is changed. The computed amplitude and phase frequency spectra of the EM field components demonstrate that the quasi-static approach produces inaccurate results at frequencies higher than 1 MHz, and that, in particular, it leads to underestimating the EM field strength. Finally, it is also shown that at a frequency equal to or greater than 10 MHz excellent results in terms of accuracy may be obtained by using the high-frequency asymptotic forms of the exact solutions.

1. INTRODUCTION

It is well known that measuring the EM field produced by a current-carrying insulated wire loop lying on the surface of a terrestrial area makes it possible to acquire information about the subsurface structure [1–6]. In particular, when the soil properties do not vary

Received 7 June 2010, Accepted 8 July 2010, Scheduled 13 July 2010
Corresponding author: M. Parise (m.parise@unicampus.it).

spatially, the presence of shallow buried objects such as mines, metals, or mineral resources can be detected by the departure of the recorded time- or frequency-domain experimental data from the theoretical results obtained regarding the ground as a homogeneous conducting half-space [1–5, 7].

It is a common practice to compute the theoretical response curves by treating the loop source as a vertical magnetic dipole. The small loop assumption is reasonable, since the diameter of the source is in most cases small if compared to both the source-receiver distance and the free-space wavelength. A number of analytical and semi-analytical techniques have been recently developed for evaluating the time- and frequency-domain complete integral expressions for the EM field components produced by a VMD placed above the surface of a material half-space [1–6, 8–13].

In particular, closed-form solutions in the frequency-domain have been derived under the quasi-static field assumption [4, 6], that is neglecting the high-frequency effects due to the displacement currents in both the air and the ground. Such solutions constitute the preferred choice when the measurement data to be interpreted are in terms of mutual impedance between source and receiver loops (that is the voltage induced in the receiver loop per unit current flowing in the source loop [1, 5, 6, 8, 14]), but unfortunately are valid only in the low-frequency range.

In this paper, the exact closed-form expressions for the time-harmonic EM field components excited by a VMD lying on the surface of a flat and homogeneous lossy half-space are derived, with the principal aim of identifying the boundary between quasi-static and non-quasi-static frequency regions. As it frequently occurs that the whole EM prospecting system (i.e., both source and receiver) is positioned on the ground to be explored, the discussion is limited to the case where even the observation point is located on the half-space. The paper is organized as follows. In Section 2 the complete integral representations for the EM field components are cast into forms involving only known tabulated Sommerfeld Integrals. In Section 3, the derived closed-form expressions are used to compute both the amplitude- and phase-frequency spectra of the fields, and the achieved results are compared with the data provided by both the quasi-static and high-frequency formulations. It is concluded from the conducted analysis that the quasi-static formulation is valid up to 1 MHz, while it leads to underestimating the EM field strength by a factor greater than 100 for frequencies higher than 10 MHz, whereas excellent results in terms of accuracy may be obtained by using the high-frequency asymptotic forms of the exact solutions. Finally, some conclusive

remarks are drawn in Section 4.

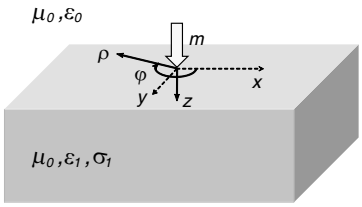

Figure 1. Sketch of a vertical magnetic dipole on a homogeneous lossy medium.

2. THEORY

Consider a VMD of moment $me^{j\omega t}$ lying on the surface of a flat, homogeneous, isotropic and linear lossy medium, as shown in Fig. 1. Due to symmetry about the axis of the dipole, a cylindrical co-ordinate system (r, φ, z) is suitably introduced. The medium is assumed to have the magnetic permeability of free space μ_0, dielectric permittivity ϵ_1 and electric conductivity σ_1. The time-harmonic analytical expressions for the non-null EM field components E_φ, H_ρ, and H_z generated on the surface of the medium can be obtained from those corresponding to source and field points located respectively at heights h and $-z$ above the medium by setting $h = 0$ and $z = 0$. Thus, with the time-harmonic factor $e^{j\omega t}$ suppressed for better clarity, the EM field components may be expressed as [2, 8, 15–17]

$$E_\varphi(\rho) = \frac{j\omega\mu_0 m}{4\pi\left(k_0^2 - k_1^2\right)} \frac{\partial}{\partial\rho} \left[F_p + F_s\right]_{\substack{z=0 \\ h=0}}, \tag{1}$$

$$H_\rho(\rho) = \frac{m}{4\pi\left(k_0^2 - k_1^2\right)} \frac{\partial}{\partial\rho} \left.\frac{\partial F_s}{\partial z}\right|_{\substack{z=0 \\ h=0}}, \tag{2}$$

$$H_z(\rho) = -\frac{m}{4\pi\left(k_0^2 - k_1^2\right)} \left(\frac{\partial^2}{\partial\rho^2} + \frac{1}{\rho}\frac{\partial}{\partial\rho}\right) \left[F_p + F_s\right]_{\substack{z=0 \\ h=0}}, \tag{3}$$

with

$$F_p(\rho, z, h) = \left(k_0^2 - k_1^2\right) \frac{e^{-jk_0 r}}{r}, \tag{4}$$

$$F_s(\rho, z, h) = \left(k_0^2 - k_1^2\right) \int_0^\infty R^{TE} e^{-u_0(h-z)} \frac{\lambda}{u_0} J_0(\lambda\rho) d\lambda, \tag{5}$$

and being $r = [\rho^2 + (h+z)^2]^{1/2}$. In the above equations, $J_0(\xi)$ is the zeroth-order Bessel function, and

$$R^{TE} = \frac{u_0 - u_1}{u_0 + u_1} \tag{6}$$

is the transverse electric plane wave reflection coefficient at z=0, with

$$u_n = (\lambda^2 - k_n^2)^{1/2}, \tag{7}$$

$$k_n = (\omega^2 \mu_n \epsilon_n + j\omega\mu_n\sigma_n)^{1/2}. \tag{8}$$

The subscripts p and s in (1)–(5) denote respectively the primary (free-space) contribution to the field, due to the VMD alone, and the secondary (scattered) contribution arising from the electric currents induced in the lossy medium. Equation (2) dictates that there does not exist a radial component for the primary magnetic field in the plane of the dipole.

In the past, because of the lack of available analytical techniques for evaluating (1)–(3), the conventional approach was to assume the hypothesis of quasi-static field, which consists of neglecting the effects of the displacement current in both the air and the ground [4–6]. The chief drawback of the solutions obtained under this assumption is that, when used for acquiring information about the ground subsurface, they do not permit to interpret high-frequency measurement data. To overcome this limitation, in this paper the exact closed-form expressions for the EM field components are derived through a rigorous analytical integration procedure. Since expression (4) for F_p is in explicit form, the problem of evaluating E_φ, H_ρ, and H_z reduces to that of calculating the secondary terms F_s and $\partial F_s/\partial z$ for z=h=0. Throughout the analysis the dependences of the field quantities upon ρ, z, and h will be omitted for notational simplicity.

As u_n^2=λ^2−k_n^2, multiplying the numerator and denominator of (6) by $u_0 - u_1$ leads to

$$R^{TE} = \frac{(u_0 - u_1)^2}{k_1^2 - k_0^2} = \frac{2\lambda^2 - 2u_0u_1 - k_0^2 - k_1^2}{k_1^2 - k_0^2}, \tag{9}$$

which, substituted into (5), yields

$$F_s = F_s^I + F_s^{II}, \tag{10}$$

where

$$F_s^I = -\int_0^\infty \left(2\lambda^2 - k_0^2 - k_1^2\right) e^{-u_0(h-z)} \frac{\lambda}{u_0} J_0(\lambda\rho) d\lambda, \tag{11}$$

$$F_s^{II} = 2\int_0^\infty u_1 e^{-u_0(h-z)} \lambda J_0(\lambda\rho) d\lambda. \tag{12}$$

Use of the identity [18]

$$\lambda^2 J_0(\lambda\rho) = -\left(\frac{\partial^2}{\partial\rho^2} + \frac{1}{\rho}\frac{\partial}{\partial\rho}\right) J_0(\lambda\rho), \tag{13}$$

and the relation

$$u_1 = \frac{u_1^2}{u_1} = \frac{\lambda^2 - k_1^2}{u_1}, \tag{14}$$

makes it possible to rewrite (11) and (12) as

$$\begin{aligned} F_s^I &= \left(2\frac{\partial^2}{\partial\rho^2} + \frac{2}{\rho}\frac{\partial}{\partial\rho} + k_0^2 + k_1^2\right)\int_0^\infty e^{-u_0(h-z)}\frac{\lambda}{u_0}J_0(\lambda\rho)d\lambda \\ &= \left(2\frac{\partial^2}{\partial\rho^2} + \frac{2}{\rho}\frac{\partial}{\partial\rho} + k_0^2 + k_1^2\right)\frac{e^{-jk_0R}}{R}, \end{aligned} \tag{15}$$

$$F_s^{II} = -2\left(\frac{\partial^2}{\partial\rho^2} + \frac{1}{\rho}\frac{\partial}{\partial\rho} + k_1^2\right)\int_0^\infty e^{-u_0(h-z)}\frac{\lambda}{u_1}J_0(\lambda\rho)d\lambda, \tag{16}$$

being $R = [\rho^2 + (h-z)^2]^{1/2}$.

Notice that casting (11) and (12) into the forms (15) and (16) is allowed to the extent that a derivative of arbitrary order with respect to ρ can be moved outside the integrals. It reads

$$\int_0^\infty e^{-u_0(h-z)} f(\lambda)\frac{\partial^l J_0(\lambda\rho)}{\partial\rho^l}d\lambda = \frac{\partial^l}{\partial\rho^l}\int_0^\infty e^{-u_0(h-z)} f(\lambda)J_0(\lambda\rho)d\lambda \tag{17}$$

where $f(\lambda)$ is equal to λ/u_n $(n = 0, 1)$. The above interchange of derivative and integral is justified in virtue of the continuous dominated convergence theorem (CDCT) [19, Chap. 19], because the function

$$\left|e^{-u_0(h-z)} f(\lambda)\frac{\partial^l J_0(\lambda\rho)}{\partial\rho^l}\right| = e^{-\Re\{u_0\}(h-z)}\left|f(\lambda)\frac{\partial^l J_0(\lambda\rho)}{\partial\rho^l}\right| \tag{18}$$

is integrable over $[0, \infty)$ for all $\rho{>}0$ and for all $l{\geq}0$, as it exponentially decays with increasing λ.

Since it results

$$\left[\frac{e^{-jk_0R}}{R}\right]_{\substack{z=0\\h=0}} = \left[\frac{e^{-jk_0r}}{r}\right]_{\substack{z=0\\h=0}} = \frac{e^{-jk_0\rho}}{\rho}, \tag{19}$$

from (15) in conjunction with (4) it can be concluded that

$$F_s^I\big|_{\substack{z=0\\h=0}} = \left(2\frac{\partial^2}{\partial\rho^2} + \frac{2}{\rho}\frac{\partial}{\partial\rho} + k_0^2 + k_1^2\right)\frac{e^{-jk_0\rho}}{\rho} = -\,F_p\big|_{\substack{z=0\\h=0}} + 2\,Q_0(\rho), \tag{20}$$

with

$$Q_n(\rho) = \left(\frac{\partial^2}{\partial\rho^2} + \frac{1}{\rho}\frac{\partial}{\partial\rho} + k_n^2\right)\frac{e^{-jk_n\rho}}{\rho} = (jk_n\rho + 1)\frac{e^{-jk_n\rho}}{\rho^3}. \tag{21}$$

On the other hand, substitution of the identity [20, No. 4, P. 7]

$$\left[\int_0^\infty e^{-u_0(h-z)}\frac{\lambda}{u_1}J_0(\lambda\rho)d\lambda\right]_{\substack{z=0\\h=0}} = \int_0^\infty \frac{\lambda}{u_1}J_0(\lambda\rho)d\lambda = \frac{e^{-jk_1\rho}}{\rho} \tag{22}$$

into (16) leads to

$$F_s^{II}\big|_{\substack{z=0\\h=0}} = -2\left(\frac{\partial^2}{\partial\rho^2}+\frac{1}{\rho}\frac{\partial}{\partial\rho}+k_1^2\right)\frac{e^{-jk_1\rho}}{\rho} = -2\,Q_1(\rho), \tag{23}$$

which can be added to (20) to give

$$F_s\big|_{\substack{z=0\\h=0}} = -\,F_p\big|_{\substack{z=0\\h=0}} + 2\left[Q_0(\rho)-Q_1(\rho)\right]. \tag{24}$$

Next, calculating the first derivative of (15) with respect to z provides

$$\frac{\partial F_s^I}{\partial z} = \left(2\frac{\partial^2}{\partial\rho^2}+\frac{2}{\rho}\frac{\partial}{\partial\rho}+k_0^2+k_1^2\right)\left[(h-z)\,(jk_0R+1)\,\frac{e^{-jk_0R}}{R^3}\right], \tag{25}$$

which implies, as a consequence,

$$\left.\frac{\partial F_s^I}{\partial z}\right|_{\substack{z=0\\h=0}} = 0, \tag{26}$$

while applying the z-derivative to (16), and then setting z and h to zero, yields

$$\left.\frac{\partial F_s^{II}}{\partial z}\right|_{\substack{z=0\\h=0}} = -2\left(\frac{\partial^2}{\partial\rho^2}+\frac{1}{\rho}\frac{\partial}{\partial\rho}+k_1^2\right)S(\rho), \tag{27}$$

with

$$S(\rho) = \left[\int_0^\infty e^{-u_0(h-z)}\frac{u_0}{u_1}\lambda J_0(\lambda\rho)d\lambda\right]_{\substack{z=0\\h=0}}. \tag{28}$$

To evaluate (28), it is convenient to multiply the numerator and denominator of the integrand by u_0 and then use (7) and (13) to obtain

$$\begin{aligned} S(\rho) &= \left[\int_0^\infty e^{-u_0(h-z)}\frac{\lambda^2-k_0^2}{u_0u_1}\lambda J_0(\lambda\rho)d\lambda\right]_{\substack{z=0\\h=0}} \\ &= -\left(\frac{\partial^2}{\partial\rho^2}+\frac{1}{\rho}\frac{\partial}{\partial\rho}+k_0^2\right)\int_0^\infty\frac{\lambda}{u_0u_1}J_0(\lambda\rho)\,d\lambda. \end{aligned} \tag{29}$$

The integral on the right-hand side of (29) can be evaluated by using [20, No. 17, P. 8]. It results

$$\int_0^\infty\frac{\lambda}{u_0u_1}J_0(\lambda\rho)\,d\lambda = K_0\left(\alpha\rho\right)I_0\left(\beta\rho\right), \tag{30}$$

where $I_0(\xi)$ and $K_0(\xi)$ are the zeroth-order modified Bessel functions of the first and second kind, respectively, and

$$\alpha = \frac{1}{2} j\left(k_1 + k_0\right), \quad \beta = \frac{1}{2} j\left(k_1 - k_0\right). \tag{31}$$

Combining (27), (29), and (30) leads to the equation

$$\begin{aligned}
\left.\frac{\partial F_s^{II}}{\partial z}\right|_{\substack{z=0\\h=0}} &= 2\left(\frac{\partial^2}{\partial\rho^2}+\frac{1}{\rho}\frac{\partial}{\partial\rho}+k_1^2\right)\left(\frac{\partial^2}{\partial\rho^2}+\frac{1}{\rho}\frac{\partial}{\partial\rho}+k_0^2\right) K_0\left(\alpha\rho\right) I_0\left(\beta\rho\right) \\
&= 2\left[\frac{\partial^4}{\partial\rho^4}+\frac{2}{\rho}\frac{\partial^3}{\partial\rho^3}+\left(-\frac{1}{\rho^2}+k_0^2+k_1^2\right)\frac{\partial^2}{\partial\rho^2}\right. \\
&\quad \left.+\left(\frac{1}{\rho^3}+\frac{k_0^2+k_1^2}{\rho}\right)\frac{\partial}{\partial\rho}+k_0^2k_1^2\right] K_0\left(\alpha\rho\right) I_0\left(\beta\rho\right),
\end{aligned} \tag{32}$$

which, after performing all the derivatives and making use of the relations

$$-2\left(\alpha^2+\beta^2\right) = k_0^2+k_1^2, \tag{33}$$

$$\left(\alpha^2-\beta^2\right) = -k_0k_1, \tag{34}$$

$$4\alpha\beta = k_0^2-k_1^2, \tag{35}$$

becomes

$$\begin{aligned}
\left.\frac{\partial F_s^{II}}{\partial z}\right|_{\substack{z=0\\h=0}} &= 4\alpha^2\beta^2\left[\frac{2}{\alpha\rho}K_1\left(\alpha\rho\right) I_0\left(\beta\rho\right)\right. \\
&\quad \left.-\frac{2}{\beta\rho}K_0\left(\alpha\rho\right) I_1\left(\beta\rho\right)-\frac{4}{\alpha\beta\rho^2}K_1\left(\alpha\rho\right) I_1\left(\beta\rho\right)\right] \\
&= 4\alpha^2\beta^2\left[K_2\left(\alpha\rho\right) I_2\left(\beta\rho\right)-K_0\left(\alpha\rho\right) I_0\left(\beta\rho\right)\right].
\end{aligned} \tag{36}$$

Substituting (24) into (1) and (3) gives rise to the radial distributions of E_φ and H_z, namely

$$E_\varphi\left(\rho\right) = \frac{j\omega\mu_0 m}{2\pi\left(k_0^2-k_1^2\right)}\left[Q_0'(\rho)-Q_1'(\rho)\right], \tag{37}$$

$$\begin{aligned}
H_z\left(\rho\right) &= -\frac{m}{2\pi\left(k_0^2-k_1^2\right)}\left[Q_0''(\rho)-Q_1''(\rho)+\frac{Q_0'(\rho)-Q_1'(\rho)}{\rho}\right] \\
&= -\frac{m}{2\pi\left(k_0^2-k_1^2\right)}\left[\hat{Q}_0\left(\rho\right)-\hat{Q}_1\left(\rho\right)\right],
\end{aligned} \tag{38}$$

being

$$Q_n'\left(\rho\right) = \frac{dQ_n\left(\rho\right)}{d\rho} = \left(k_n^2\rho^2-3jk_n\rho-3\right)\frac{e^{-jk_n\rho}}{\rho^4}, \tag{39}$$

$$Q_n''\left(\rho\right) = \frac{dQ_n'\left(\rho\right)}{d\rho} = \left(-jk_n^3\rho^3-5k_n^2\rho^2+12jk_n\rho+12\right)\frac{e^{-jk_n\rho}}{\rho^5}, \tag{40}$$

and

$$\hat{Q}_n(\rho) = Q_n''(\rho) + \frac{Q_n'(\rho)}{\rho} = (-jk_n^3\rho^3 - 4k_n^2\rho^2 + 9jk_n\rho + 9)\frac{e^{-jk_n\rho}}{\rho^5}. \quad (41)$$

Finally, the radial magnetic field component H_ρ is obtained by using (26) and (36) in (2). It is found that

$$\begin{aligned} H_\rho(\rho) &= \frac{m\alpha\beta}{4\pi}\frac{d}{d\rho}\left[K_2(\alpha\rho)I_2(\beta\rho) - K_0(\alpha\rho)I_0(\beta\rho)\right] \\ &= \frac{m}{\pi\rho}\left[\frac{\alpha^2+\beta^2}{2}K_1(\alpha\rho)I_1(\beta\rho) - \alpha\beta K_2(\alpha\rho)I_2(\beta\rho)\right]. \quad (42) \end{aligned}$$

The familiar quasi-static expressions for the fields may be obtained directly from (37), (38), and (42) by setting k_0=0. Under this condition, from (31), (39), and (41) it follows that

$$\alpha = \beta = \frac{jk_1}{2} = \frac{\gamma}{2}, \quad Q_0'(\rho) = -\frac{3}{\rho^4}, \quad \hat{Q}_0(\rho) = \frac{9}{\rho^5}, \quad (43)$$

and, as a consequence, it yields

$$E_\varphi(\rho) = -\frac{j\omega\mu_0 m}{2\pi\gamma^2\rho^4}\left[3 - \left(\gamma^2\rho^2 + 3\gamma\rho + 3\right)e^{-\gamma\rho}\right], \quad (44)$$

$$H_\rho(\rho) = \frac{m\gamma^2}{4\pi\rho}\left[K_1\left(\frac{\gamma\rho}{2}\right)I_1\left(\frac{\gamma\rho}{2}\right) - K_2\left(\frac{\gamma\rho}{2}\right)I_2\left(\frac{\gamma\rho}{2}\right)\right], \quad (45)$$

$$H_z(\rho) = -\frac{m}{2\pi\gamma^2\rho^5}\left[9 - (\gamma^3\rho^3 + 4\gamma^2\rho^2 + 9\gamma\rho + 9)e^{-\gamma\rho}\right], \quad (46)$$

that is the same equations as in [4–6].

Other useful expressions are the far-field or high-frequency approximations of (37), (38), and (42). Retaining only the higher-order powers of $k_n\rho$ [21–23] in (39) and (41), and introducing the asymptotic forms of the modified Bessel functions for large arguments [24, 8.451]

$$I_n(\beta\rho) \approx \frac{e^{\beta\rho} + (-1)^n je^{-\beta\rho}}{\sqrt{2\pi\beta\rho}}, \quad (47)$$

$$K_n(\alpha\rho) \approx \sqrt{\frac{\pi}{2\alpha\rho}}e^{-\alpha\rho}, \quad (48)$$

in (42), make it possible to obtain the formulas

$$E_\varphi(\rho) = \frac{j\omega\mu_0 m}{2\pi\left(k_0^2 - k_1^2\right)\rho^2}\left(k_0^2 e^{-jk_0\rho} - k_1^2 e^{-jk_1\rho}\right), \quad (49)$$

$$H_\rho(\rho) = \frac{m}{2\pi\sqrt{k_0^2 - k_1^2\rho^2}}\left(k_0^2 e^{-jk_0\rho} - jk_1^2 e^{-jk_1\rho}\right), \quad (50)$$

$$H_z(\rho) = \frac{jm}{2\pi\left(k_0^2 - k_1^2\right)\rho^2}\left(k_0^3 e^{-jk_0\rho} - k_1^3 e^{-jk_1\rho}\right), \quad (51)$$

the last of which is identical to the expression given by Kong [25, Sec. 4.9, No. 19].

3. RESULTS AND DISCUSSION

The exact formulas (37), (38), and (42) are applied to the computation of the EM field components generated on the top surface of a medium with ϵ_1=10 ϵ_0 at distance ρ = 100 m from a unit-moment VMD. At first, the amplitudes of E_φ, H_ρ, and H_z versus frequency are computed for two different values of the conductivity σ_1. The obtained results, depicted in Figs. 2–4, are compared with the data provided by the

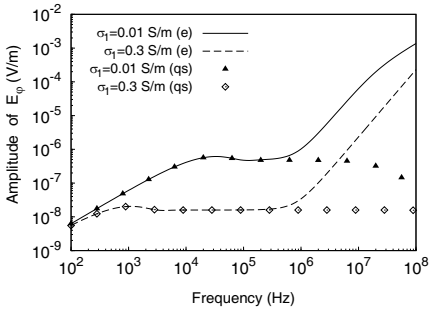

Figure 2. Amplitude of E_φ-field versus frequency, computed by applying the quasi-static (qs) and exact (e) solutions.

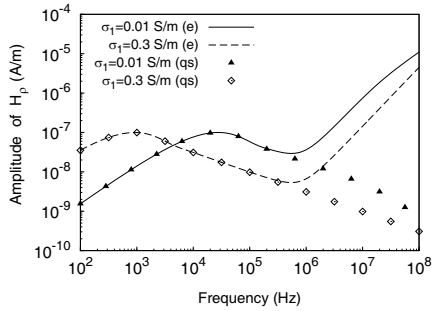

Figure 3. Amplitude of H_ρ-field versus frequency, computed by applying the quasi-static (qs) and exact (e) solutions.

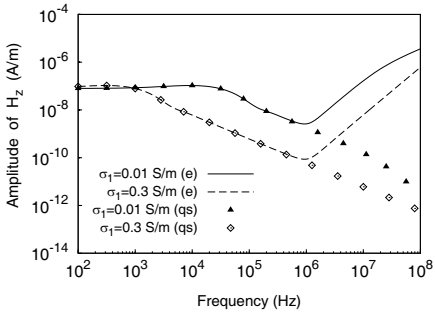

Figure 4. Amplitude of H_z-field versus frequency, computed by applying the quasi-static (qs) and exact (e) solutions.

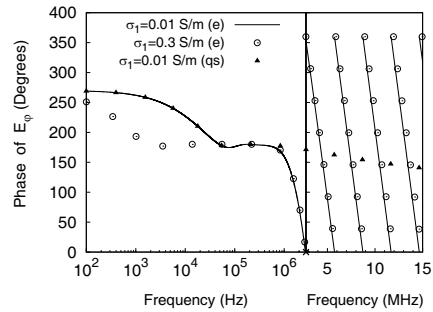

Figure 5. Phase of E_φ-field versus frequency, computed by applying the quasi-static (qs) and exact (e) solutions.

quasi-static solutions (44)–(46). It should be noted that each exact curve and its quasi-static approximation are overlapping in the low-frequency range up to about 1 MHz. Starting from such frequency, the two trends diverge. From the analysis of the plotted curves it is also seen that at frequencies higher than 10 MHz the quasi-static approach leads to underestimating the amplitudes of the field components by more than two orders of magnitudes. Furthermore, exact curves exhibit an abrupt slope increase near 1 MHz, which is followed by a positive-slope high-frequency asymptotic behavior. On the contrary, the quasi-static profiles maintain the same slope as below 1 MHz, and their high-frequency asymptotes are almost horizontal. Figs. 2–4 also point out that the high-frequency asymptotes of the amplitude curves shift downward as σ_1 increases.

Significant conclusions can be also drawn from the analysis of Figs. 5–7, which illustrate the behavior of the phase angle of E_φ, H_ρ, and H_z as a function of frequency. First, it is confirmed that the quasi-static assumption is valid up to some MHz. Second, it should be noticed that all the phase curves undergo a transition from a non-periodic to a periodic-like behavior when entering the non-quasi-static frequency region. In order to better distinguish successive cycles of the periodic trend, the logarithmic frequency scale is replaced with a linear scale starting from the abscissa value marked with a cross ($<$ 3 MHz). The basic pattern that repeats itself in the periodic structure is approximately a line segment. This means that, for frequencies higher than 3 MHz, the real and imaginary parts of the EM field components oscillate harmonically with increasing frequency. Moreover, the plotted curves demonstrate that at 100 kHz and over the phase angle is weakly affected by a variation of the conductivity σ_1.

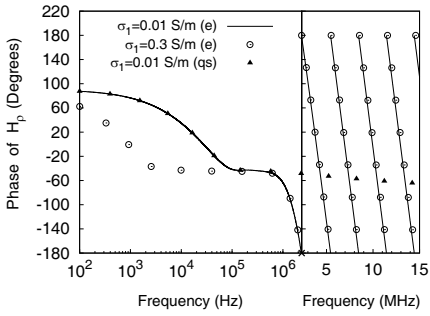

Figure 6. Phase of H_ρ-field versus frequency, computed by applying the quasi-static (qs) and exact (e) solutions.

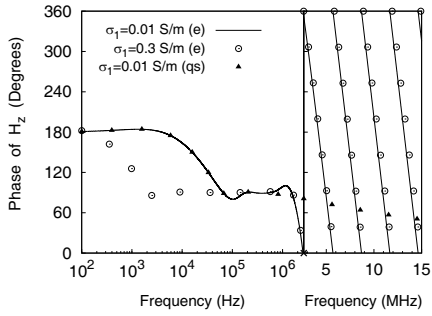

Figure 7. Phase of H_z-field versus frequency, computed by applying the quasi-static (qs) and exact (e) solutions.

It is possible to show that the frequency range of validity of the quasi-static approximation cannot be significantly affected by a variation of the dielectric permittivity ϵ_1 of the half-space. In fact, assuming $\sigma_1 = 0.01\,\mathrm{S/m}$, at a frequency lower than 1 MHz it results $\sigma_1/\omega > 180\,\epsilon_0 \gg \epsilon_{r_1}\epsilon_0$, as in real applications the relative permittivity of the ground ϵ_{r_1} is at most equal to 20. This means that the wavenumber k_1 has effectively a very weak dependence on ϵ_1. As a consequence, at less than 1 MHz both the exact and quasi-static

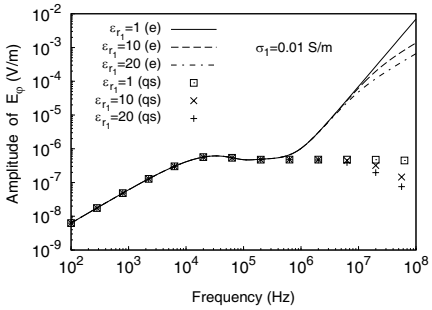

Figure 8. Amplitude of E_φ-field versus frequency, computed by applying the quasi-static (qs) and exact (e) solutions. The relative dielectric permittivity ϵ_{r_1} is taken as a parameter.

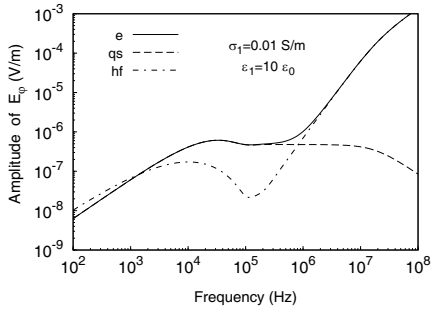

Figure 9. Amplitude of E_φ-field versus frequency, computed by applying the quasi-static (qs), high-frequency (hf), and exact (e) solutions.

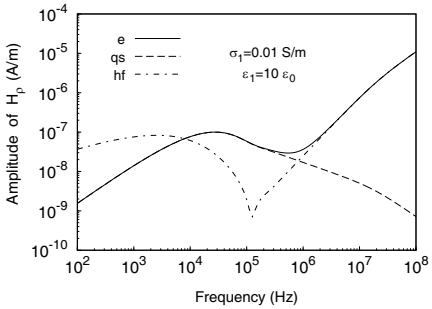

Figure 10. Amplitude of H_ρ-field versus frequency, computed by applying the quasi-static (qs), high-frequency (hf), and exact (e) solutions.

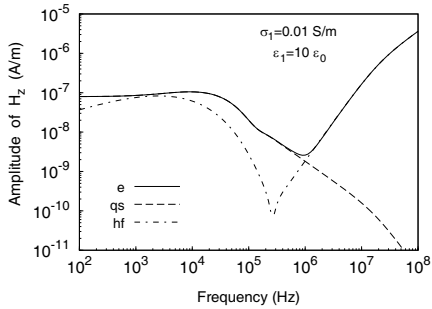

Figure 11. Amplitude of H_z-field versus frequency, computed by applying the quasi-static (qs), high-frequency (hf), and exact (e) solutions.

curves do not suffer significant changes with varying ϵ_{r_1} between 1 and 20, and the frequency at which the two trends start to diverge also remains unaltered. This aspect is pointed out in Fig. 8, where the various amplitude-frequency spectra of E_φ corresponding to different values of ϵ_{r_1} are seen to be overlapping in the low-frequency range up to about 10 MHz.

Finally, Figs. 9–11 illustrate the amplitude-frequency spectra of the fields computed by applying the exact, the high-frequency, and the quasi-static formulations. What emerges from the analysis of the plotted curves is that the transition zone where both the approximations lead to inaccurate results is a small frequency interval in a neighbourhood of 1 MHz.

4. CONCLUSION

The closed-form exact expressions for the radial distributions of the EM field components excited by a VMD on the surface of a material half-space have been derived in this paper. The expressions are in terms of exponential funtions (E_φ- and H_z-field) and modified Bessel functions (H_ρ-field), and result from a rigorous analytical procedure that has allowed to cast the complete integral representations for the time-harmonic EM field components into forms involving only known tabulated Sommerfeld Integrals. As exact solutions, they are valid in the quasi-static as well as non-quasi-static frequency regions and, unlike the previously published quasi-static solutions, make it possible to interpret high-frequency measurement data acquired for probing interiors of terrestrial areas. Numerical results are presented to outline the frequency range of validity of the quasi-static approximation. The obtained results show that the amplitude- and phase-frequency spectra of E_φ, H_ρ, and H_z computed by applying the quasi-static approach deviate from the exact ones starting from the frequency of about 1 MHz. Moreover, at frequencies higher than 10 MHz quasi-static solutions give rise to an underestimation of the amplitudes of the fields by more than two orders of magnitudes, while high-frequency asymptotic forms of the exact solutions yield very accurate results.

REFERENCES

1. Simons, N. R. S., A. Sebak, and G. E. Bridges, "Application of the TLM method to half-space and remote-sensing problems," *IEEE Trans. Geosci. Remote Sensing*, Vol. 33, No. 3, 759–767, 1995.
2. Rafi, G. Z., R. Moini-Mazandaran, and R. Faraji-Dana, "A new time domain approach for analysis of vertical magnetic

dipole radiation in front of lossy half-space," *Progress In Electromagnetics Research*, Vol. 29, 57–68, 2000.

3. Cui, T. J., W. C. Chew, A. A. Aydiner, D. L. Wright, D. W. Smith, and J. D. Abraham, "Numerical modeling of an enhanced very early time electromagnetic (VETEM) prototype system," *IEEE Antennas Propagat. Magazine*, Vol. 42, No. 2, 17–27, 2000.
4. Zhdanov, M. S., *Geophysical Electromagnetic Theory and Methods*, Elsevier, Amsterdam, 2009.
5. Wait, J. R., "Mutual electromagnetic coupling of loops over a homogeneous ground," *Geophysics*, Vol. 20, No. 3, 630–637, 1955.
6. Das, I., "Effects of soil electromagnetic properties on metal detectors," *IEEE Trans. Geosci. Remote Sensing*, Vol. 44, No. 6, 1444–1453, 2006.
7. Cui, T. J., W. C. Chew, X. X. Yin, and W. Hong, "Study of resolution and super resolution in electromagnetic imaging for half-space problems," *IEEE Trans. Antennas Propagat.*, Vol. 52, No. 6, 1398–1411, 2004.
8. Singh, N. P. and T. Mogi, "Electromagnetic response of a large circular loop source on a layered earth: A new computation method," *Pure and Applied Geophysics*, Vol. 162, No. 1, 181–200, 2005.
9. Van der Pol, B., "On discontinuous electromagnetic waves and the occurrence of a surface wave," *IRE Trans. Antennas Propagat.*, Vol. 4, 288–293, 1956.
10. Nikoskinen, K. I., "Time-domain study of half-space transmission problem with vertical and horizontal dipoles," *IEEE Trans. Antennas Propagat.*, Vol. 41, No. 10, 1399–1407, 1993.
11. Nikoskinen, K. I. and I. V. Lindell, "Time-domain analysis of the sommerfeld VMD problem based on the exact image theory," *IEEE Trans. Antennas Propagat.*, Vol. 38, No. 2, 241–250, 1990.
12. Haddad, H. and D. C. Cheng, "Transient electromagnetic field generated by a vertical dipole on the surface of a dissipative earth," *Radio Science*, Vol. 16, No. 2, 169–177, 1981.
13. Parise, M. and S. Cristina, "High-order electromagnetic modeling of shortwave inductive diathermy effects," *Progress In Electromagnetics Research*, Vol. 92, 235–253, 2009.
14. Kalaee, P. and J. Rashed-Mohassel, "Investigation of dipole radiation pattern above a chiral media using 3D BI-FDTD approach," *Journal of Electromagnetic Waves and Applications*, Vol. 23, No. 1, 75–86, 2009.
15. Milligan, T. A., *Modern Antenna Design*, Wiley-IEEE Press,

Hoboken, NJ, 2005.

16. Chew, W. C., *Waves and Fields in Inhomogeneous Media*, Van Nostrand Reinhold, New York, 1990.
17. Felsen, L. B. and N. Marcuvitz, *Radiation and Scattering of Waves*, IEEE Press, Piscataway, NJ, 1994.
18. Abramowitz, M. and I. A. Stegun, *Handbook of Mathematical Functions with Formulas, Graphs, and Mathematical Tables*, Dover, New York, 1964.
19. Priestley, H. A., *Introduction to Integration*, Oxford University Press, Oxford, 1997.
20. Erdelyi, A., *Tables of Integral Transforms*, Vol. 2, McGraw-Hill, New York, 1954.
21. Liu, L., K. Li, and W.-Y. Pan, "Electromagnetic field from a vertical electric dipole in a four-layered region," *Progress In Electromagnetics Research B*, Vol. 8, 213–241, 2008.
22. Lu, Y. L., Y.-L. Wang, Y. H. Xu, and K. Li, "Electromagnetic field of a horizontal electric dipole buried in a four-layered region," *Progress In Electromagnetics Research B*, Vol. 16, 247–275, 2009.
23. Illahi, A., M. Afzaal, and Q. A. Naqvi, "Scattering of dipole field by a perfect electromagnetic conductor cylinder," *Progress In Electromagnetics Research Letters*, Vol. 4, 43–53, 2008.
24. Gradshteyn, I. S. and I. M. Ryzhik, *Table of Integrals, Series, and Products*, 7th edition, Academic Press, New York, 2007.
25. Kong, J. A., *Electromagnetic Wave Theory*, John Wiley & Sons, New York, 1986.